JURNAL BIOSENSE
Jurnal Penelitian Biologi dan Terapannya
Volume 9 No. 1, Januari 2026, Hal 171 - 194 E-ISSN: 2622 - 6286

DNA-3-METHYLADENINE GLYCOSYLASE AS CANCER TARGET PROTEIN OF GOSSYPOL DERIVATIVES: A COMPUTATIONAL PHARMACOLOGY ANALYSIS

Muhammad Faisal*, Ilham Hariaji
Department of Pharmacology, Faculty of Medicine, Universitas Muhammadiyah Sumatera Utara, Medan 20217 Indonesia
*Corresponding author e-mail: muhammadfaisal@umsu.ac.id

Abstract

Gossypol, a natural polyphenolic compound derived from Gossypium species, has demonstrated broad anticancer activity; however, its clinical application is limited by poor pharmacokinetic properties and toxicity. This study employed an integrated computational pharmacology approach to evaluate gossypol and its derivatives, identify potential cancer-related target proteins, and elucidate their molecular interactions. ADMET profiling, cytotoxicity prediction, target identification, protein expression and prognostic analysis, and molecular docking were systematically performed. Several gossypol derivatives, particularly anhydrogossypol and gossypolone, exhibited improved drug-likeness, reduced predicted toxicity, favorable anticancer activity, and enhanced selectivity toward cancer cells compared with the parent compound. PASS-based target prediction consistently identified DNA-3-methyladenine glycosylase (MPG), a key enzyme in the base excision repair pathway, as a high-confidence molecular target. Clinical relevance analysis revealed that elevated MPG expressions were associated with unfavorable prognosis and were highly expressed across multiple cancer types, including colorectal, breast, and lung cancers. Molecular docking demonstrated strong binding affinities of selected derivatives within the MPG active site, involving conserved and functionally important residues such as TYR-127, TYR-165, CYS-167, and ARG-182. These findings suggest that gossypol derivatives may exert anticancer effects by modulating MPG-mediated DNA repair mechanisms. Overall, this study highlights MPG as a promising therapeutic target and supports further experimental investigation of optimized gossypol derivatives as potential anticancer agents.

Keywords: ***Cancer target; Computational pharmacology; DNA-3-methyladenine glycosylase; Gossypol derivatives***

1. INTRODUCTION

Cancer continues to pose a significant global health burden and is persistently ranked as the second leading cause of death worldwide (Bray et al., 2024). Despite significant advances in chemotherapy and targeted therapy, treatment resistance and systemic toxicity remain major challenges. Pharmacological identification of novel molecular targets and the development of compounds with increasing pharmacological

effects are critical aspects for advancing cancer treatment strategies (Koirala & DiPaola, 2024).

Gossypol is a natural compound from cotton plants (Gossypium *spp*., **Figure 1**) which is classified as phenolic aldehyde. These derivatives have been extensively reported for their broad-spectrum anticancer activity. Prior studies have demonstrated its ability to hinder tumor cell proliferation and cancer progression in various cancer types, including breast (Xiong et al., 2017), colorectal (Lan et al., 2015), lung (Wang et al., 2018), liver (Elkattan et al., 2025), prostate (Lin, 2009), and pancreatic cancers (Lee et al., 2022). Nevertheless, the clinical application of gossypol has been limited by unfavorable pharmacokinetic properties and toxicity (Gadelha et al., 2014; Sun et al., 2025). To overcome these limitations, several gossypol derivatives have been synthesized, showing structural alterations that may enhance selectivity, bioavailability, and target specificity.

Figure 1. Cotton plants (https://www.stuartxchange.org/BulakCotton)

DNA repair pathways play a crucial role in maintaining genomic stability. Abnormal state of these pathways is closely associated with cancer development and progression (Alhmoud et al., 2020). DNA-3-methyladenine glycosylase (MPG) is a key enzyme involved in the base excision repair (BER) pathway which is responsible for fixing the alkylated and damaged DNA bases (Kladova & Kuznetsova, 2025). Overexpression of MPG has been implicated in tumorigenesis, cancer cell survival, and

therapeutic resistance, highlighting its potential as a molecular target in cancer therapy (Agnihotri et al., 2014).

Although the anticancer activity of gossypol has been classically attributed to its role as a BH3 mimetic that inhibits anti-apoptotic Bcl-2 family proteins, thereby activating mitochondrial-dependent apoptotic pathways (Huang et al., 2010; Wong et al., 2012; Ni et al., 2013; Sadahira et al., 2014). While this mechanism has been extensively documented, it does not fully account for the diverse anticancer efficacy of gossypol derivatives against various cancers. On the other hand, targeting MPG represents a basically distinct therapeutic strategy, due to MPG functions associated with DNA damage recognition and BER, contributing to genomic maintenance and cancer cell survival under genotoxic stress (Kladova & Kuznetsova, 2025). Unlike Bcl-2 inhibition, which primarily induces apoptosis, MPG modulation may disrupt DNA repair capacity and metabolic stress adaptation, potentially sensitizing cancer cells to endogenous damage and therapeutic agents. This mechanistic divergence marks MPG as an underexplored molecular target that expands the pharmacological landscape of goysspol beyond its established anticancer mechanism.

Computational pharmacology has emerged as a powerful approach for accelerating drug discovery by integrating *in silico* prediction of pharmacokinetic properties, biological activity, and molecular interactions (Wu et al., 2020). This present study comprehensively utilized computational pharmacology framework to predict gossypol and its derivatives, identify promising cancer-related target proteins, and investigate the interaction of these active compounds with MPG. By integrating ADMET profiling, anticancer activity prediction, target identification, expression and prognostic analysis, and molecular docking, this work aims to provide mechanistic insights into the anticancer potential of gossypol derivatives and foster MPG as a promising therapeutic target for further experimental investigation.

2. METHODOLOGY

2.1 ADMET profiling

The ADMET profiles of gossypol and its derivatives were predicted using some online platforms including ADMETLAB 3.0 (https://admetlab3.scbdd.com/) and ProTox 3.0 (https://tox.charite.de/protox3/). Simplified Molecular-Input Line-Entry System (SMILES) of each compound was assigned as input for this study (**Table 1**). Physicochemical descriptors such as molecular weight (MW), number of hydrogen bond acceptors (nHA), number of hydrogen bond donors (nHD), octanol/water partition coefficient (LogP), and topological polar surface area (TPSA) were calculated to find out whether the compounds were accepted or rejected by Lipinski's rule of five (RO5). Human intestinal absorption (HIA) was predicted and expressed as percentage absorption, with values ≥ 30% considered indicative of moderate to high oral absorption. Distribution properties were estimated by predicting the steady-state volume of distribution (VDss, L/kg). Metabolic stability was estimated in predicted human liver microsomal (HLM) stability, reported as intrinsic clearance time (≤ 30 min indicating low metabolic stability). Excretion was evaluated by predicting plasma clearance (CLplasma, mL/min/kg). Meanwhile, toxicity was evaluated by predicting acute oral toxicity, expressed as the median lethal dose (LD_{50}, mg/kg) (Banerjee et al., 2024; Fu et al., 2024).

2.2 Predictive cytotoxicity level, selectivity index, and target protein

The cytotoxicity and target protein of gossypol and its derivatives was predicted using the Way2Drug web platform (https://way2drug.com/clc-pred/), an online computational tool for biological activity estimation based on chemical structure. This prediction is based on quantitative structure-activity relationship (QSAR) models trained on experimentally validated cytotoxicity data. SMILES of each compound was exploited as an input descriptor. The output of this prediction was predictive half-maximal inhibitory concentration (pIC_{50}) and predicted selectivity index (SI) by dividing pIC_{50} of cancer cells with pIC_{50} of non-cancerous cells. Additionally, target

protein candidates of gossypol and its derivatives output were active probabilities (Pa), inactive probabilities (Pi), and invariant accuracy of prediction (IAP) (Lagunin et al., 2023, 2024).

2.3 Protein expression and prognostic relevance analysis

After finding the predictive cancer target protein, we evaluated its protein expression pattern and prognostic relevance through Human Protein Atlas (HPA) database (https://www.proteinatlas.org/) which is included as publicly available data. Cancer-specific expression was evaluated by comparing expression levels across multiple tumor types. Prognostic analysis was performed using the survival analysis tools provided by HPA, which assess the relationship among protein expression and overall patient survival. Patients were stratified into high- and low-expression groups based on median DNA-3-methyladenine glycosylase (MPG) expression, and survival outcomes were visualized using Kaplan-Meier plots. Statistical significance was determined by log-rank testing as provided by the database.

2.4 Molecular docking

2.4.1 Protein preparation

The three-dimensional crystal structure of human MPG was retrieved from the Protein Data Bank RCSB (https://www.rcsb.org) with code identified 7XFH. Protein preparation involved removal of water molecules, and non-essential heteroatoms. Polar hydrogen atoms were added, and the protein structure was optimized to ensure suitable geometry for docking analysis using AutoDock Tools (ADT) version 1.5.7 (Morris *et al*., 2000). Due to an absence of co-crystallized ligand on MPG protein structure and FDA-approved MPG inhibitor, we performed the molecular docking with sunitinib (CID: 5329102). Moreover, as previously stated, sunitinib was able to inhibit the activity of alkyladenine DNA glycosylase (Song et al., 2023).

2.4.2 Ligand preparation

Structure data file format (SDF) chemical structures of gossypol and its derivatives were obtained from the PubChem database (https://pubchem.ncbi.nlm.nih.gov/) . All

SDF files were converted into three-dimensional formats using CACTUS online chemical translator (https://cactus.nci.nih.gov/translate/) and subjected to geometry optimization and energy minimization with Merck Molecular Forcefield 94 (MMFF94) and steepest descent algorithm in the Avogadro software (Hanwell et al., 2012).

2.4.3 Grid and docking parameterization

Prior to setting up the docking parameter, the grid box was adjusted as the binding pocket position and size. The binding pocket position was predicted using PrankWeb online platform (https://prankweb.cz/) and obtained the fix position at 143.55 × 109.56 × 139.68 $Å^3$ and the size was 60×60×60 $Å^3$. Subsequently, the docking parameter was setting up the genetic algorithm within 15 running and population size as much as 150 population (Faisal et al., 2024).

2.4.4 Running molecular docking and results interpretation

Molecular docking was performed in AutoDock Tools version 1.5.7 using AMD Ryzen 5-5500U with 12 cores and AMD Radeon Graphics Unit. This docking study found both binding affinity and inhibition constant. The docking poses were visualized in Biovia Discovery Studio (https://discover.3ds.com/discovery-studio-visualizer-download) for 2D and PyMOL (Schrödinger and DeLano, 2020). Not only binding affinity and inhibition constant, but also molecular interactions were analyzed to identify key hydrogen bonds, hydrophobic contacts, and π-π interactions among MPG and the docked compounds.

3. RESULTS AND DISCUSSION

3.1 Gossypol and its derivatives structure elucidation and ADMET prediction

The chemical structures and molecular characteristics of gossypol and its eight derivatives are summarized in **Table 1**. Gossypol ($C_{30}H_{30}O_8$) is a naturally occurring polyphenolic binaphthyl dialdehyde isolated from *Gossypium* species and is known for its broad biological activities, including anticancer effects (Lin, 2009; Lan et al., 2015; Xiong et al., 2017; Wang et al., 2018; Lee et al., 2022; Elkattan et al., 2025). Structural

JURNAL BIOSENSE
Jurnal Penelitian Biologi dan Terapannya
Volume 9 No. 1, Januari 2026, Hal 171 - 194 E-ISSN: 2622 - 6286

derivatization of gossypol through methoxylation, deoxygenation, oxidative modification, and dimer cleavage resulted in compounds with altered molecular weights, polarity, and functional groups (Miller & Adams, 1937; Bell et al., 1975; Stipanovic et al., 1975; Dao, 2000; Wei, Rega, et al., 2009; Wei et al., 2010). These modifications are expected to influence membrane permeability, metabolic stability, and molecular target interactions (Saraswat et al., 2022).

Hemigossypol and its analogs possess approximately half the molecular weight of the parent compound (gossypol), a feature considered advantageous for drug development due to improved compliance with drug-likeness criteria (Bell et al., 1975; Lipinski et al., 2012). Methoxylated derivatives such as 6-methoxygossypol and 6,6′-methoxygossypol reduce phenolic hydrogen bond donors and increase lipophilicity, which may enhance bioavailability (Stipanovic et al., 1975; Lipinski et al., 2012).

Table 1. Gossypol and its derivatives CID, chemical formula, structure and references

No	Compound Name [CID]	Formula	Structure	SMILES
1	Gossypol [35053]	$C_{30}H_{30}O_8$	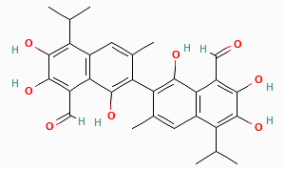	CC1=CC2=C(C(=C(C(=C2C(C)C)O)O)C=O)C(=C1C3=C(C4=C(C=C3C)C(=C(C(=C4C=O)O)O)C(C)C)O)O
2	6-Methoxygossypol [3085061]	$C_{31}H_{32}O_8$	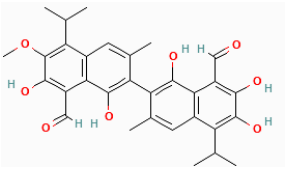	CC1=CC2=C(C(=C(C(=C2C(C)C)O)O)C=O)C(=C1C3=C(C4=C(C=C3C)C(=C(C(=C4C=O)O)OC)C(C)C)O)O
3	Hemigossypol [115300]	$C_{15}H_{16}O_4$	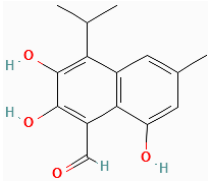	CC1=CC2=C(C(=C1)O)C(=C(C(=C2C(C)C)O)O)C=O
4	6,6'-Methoxygossypol [375713]	$C_{32}H_{34}O_8$	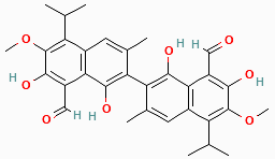	CC1=CC2=C(C(=C(C(=C2C(C)C)OC)O)C=O)C(=C1C3=C(C4=C(C=C3C)C(=C(C(=C4C=O)O)OC)C(C)C)O)O

JURNAL BIOSENSE
Jurnal Penelitian Biologi dan Terapannya
Volume 9 No. 1, Januari 2026, Hal 171 - 194 E-ISSN: 2622 - 6286

No	Compound Name [CID]	Formula	Structure	SMILES
5	6-Methoxyhemigossypol [623685]	$C_{16}H_{18}O_4$	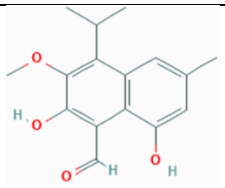	CC1=CC2=C(C(=C1)O)C(=C(C(=C2C(C)C)OC)O)C=O
6	6-Deoxyhemigossypol [618501]	$C_{15}H_{16}O_3$	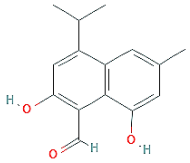	CC1=CC2=C(C(=C1)O)C(=C(C=C2C(C)C)O)C=O
7	Anhydrogossypol [135426832]	$C_{30}H_{26}O_6$	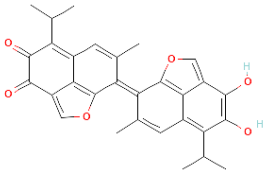	CC\\1=CC2=C(C(=C(C3=COC(=C23)/C1=C/4\\C(=CC5=C(C(=O)C(=O)C6=COC4=C56)C(C)C)C)O)O)C(C)C
8	Apogossypol [454878]	$C_{28}H_{30}O_6$	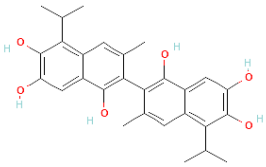	CC1=CC2=C(C(=C(C=C2C(=C1C3=C(C4=CC(=C(C(=C4C=C3C)C(C)C)O)O)O)O)O)C(C)C
9	Gossypolone [197045]	$C_{30}H_{26}O_{10}$	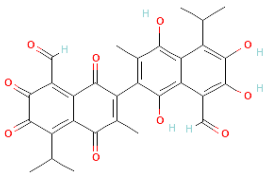	CC1=C(C(=C2C(=C(C(=C(C2=C1O)C(C)C)O)O)C=O)O)C3=C(C(=O)C4=C(C(=O)C(=O)C(=C4C3=O)C=O)C(C)C)C

Predicted ADMET properties are presented in **Table 2**. Gossypol violated Lipinski's rule of five due to its high molecular weight, excessive hydrogen bond donors, and large polar surface area, consistent with previous reports describing its limited clinical applicability (Lipinski et al., 2012; Šudomová & Hassan, 2022). In contrast, most derivatives complied with Lipinski criteria, indicating improved oral drug-likeness.

All compounds demonstrated acceptable predicted human intestinal absorption (HIA ≥ 30%), except gossypolone, which showed reduced absorption likely due to its elevated TPSA (>180 Å²) (Veber et al., 2002). Volume of distribution (VDss) values for all compounds were within the optimal pharmacokinetic range (0.04–20 L/kg), suggesting adequate tissue penetration (Ahmad et al., 2023).

Most derivatives were predicted to be unstable in human liver microsomes (HLM ≤ 30 min), indicating rapid metabolism; however, gossypolone displayed improved microsomal stability (>30 min) (Liu et al., 2015). Predicted plasma clearance values ranged from low to moderate, while acute toxicity predictions showed a marked reduction in toxicity for modified derivatives compared to gossypol, particularly for 6-methoxyhemigossypol and 6,6'-methoxygossypol, which were classified as toxicity classes V-VI (Shah et al., 2020; Banerjee et al., 2024).

Collectively, these ADMET predictions suggest that structural modification of gossypol substantially improves its pharmacokinetic feasibility and safety profile, partially overcoming the intrinsic drug-likeness limitations of the parent compound. Importantly, the combination of acceptable absorption, tissue distribution, and reduced predicted toxicity fosters the suitability of selected gossypol derivatives for further biological evaluation. These findings provide a pharmacokinetic rationale for prioritizing specific derivatives as lead candidates for subsequent anticancer activity assessment and molecular target validation.

Table 2. ADMET profiles of gossypol and its derivatives

Compound Name	MW (g/mol)	nHA	nHD	LogP	TPSA	Lipinski Rules[a]	HIA[b]	VDss (L/kg)[c]	HLM stability[d]	CL_{plasma} (ml/min/kg)[e]	LD_{50} (mg/kg)[f]
GP	518.19	8	6	3.395	155.52	Rejected	≥ 30%	0.992	≤ 30 min	8.325	325
6-MGP	532.21	8	5	3.871	144.52	Accepted	≥ 30%	1.047	≤ 30 min	6.716	3270
HGP	260.1	4	3	2.985	77.76	Accepted	≥ 30%	1.031	≤ 30 min	9.003	1425
DMGP	546.23	8	4	4.279	133.52	Accepted	≥ 30%	1.164	≤ 30 min	5.151	3270
6-MHGP	274.12	4	2	3.886	66.76	Accepted	≥ 30%	1.279	≤ 30 min	6.222	9000
6-DHMGP	244.11	3	2	3.765	57.53	Accepted	≥ 30 %	3.737	≤ 30 min	6.341	2000
AHGP	482.17	6	2	5.017	100.88	Accepted	≥ 30 %	1.862	≤ 30 min	8.984	3200
APGP	484.99	6	6	3.534	121.38	Accepted	≥ 30 %	0.797	≤ 30 min	13.979	3000
GPO	544.20	10	4	2.42	183.34	Accepted	< 30%	0.887	> 30 min	10.144	2000
SUN	398.21	6	3	3.018	77.23	Accepted	≥ 30 %	3.297	≤ 30 min	10.722	500

[a]Lipinski Rules: MW ≤ 500, logP ≤ 5, nHA ≤ 10, nHD ≤ 5; [b]HIA: human intestinal absorption (HIA+ < 30%, HIA- ≥ 30%); [c]VDss: optimal 0.04-20 L/kg; [d]HLM: human liver microsomal (stable+ HLM > 30 min, stable- HLM ≤ 30 min); [e]CL_{plasma}: clearance plasma penetration in ml/min/kg (>15 ml/min/kg: high clearance; 5-15 ml/min/kg: moderate clearance; <5 ml/min/kg: low clearance); [f]LD_{50}: half-maximal lethal dose in mg/kg (Class I: $LD_{50} \leq 5$, Class II: $5 < LD_{50} \leq 50$, Class III: $50 < LD_{50} \leq 300$, Class IV: $50 < LD_{50} \leq 2000$, Class V: $2000 < LD_{50} \leq 5000$, and Class VI: $LD_{50} > 5000$).

3.2 Predicted cytotoxicity and selectivity index of gossypol and derivatives

The predicted antiproliferative activities (pIC_{50}) of gossypol and its derivatives against breast, colorectal, and liver cancer cell lines are summarized in **Table 3**. Overall, several derivatives exhibited comparable or superior predicted anticancer activity relative to the reference drug sunitinib, indicating that structural modification

of gossypol can enhance cytotoxic potency across multiple cancer types.

In breast cancer models, 6,6′-methoxygossypol demonstrated the highest predicted activity against ZR-75-1 cells (pIC_{50}= 6.48), exceeding both the parent compound gossypol and sunitinib. In addition, gossypolone displayed strong predicted activity against MCF-7 and T47D cells, suggesting that oxidative modification of the gossypol scaffold may enhance anticancer efficacy. In colorectal cancer models, 6,6′-methoxygossypol, apogossypol, and anhydrogossypol consistently showed elevated predicted activity, particularly against COLO205 and HCT-8 cell lines, highlighting their potential effectiveness in malignancies characterized by dysregulated survival and DNA repair pathways.

HepG2 liver cancer cells exhibited moderate predicted sensitivity to all compounds, which may reflect the high metabolic capacity of hepatic cells; nevertheless, gossypolone emerged as the most potent derivative in this model. Importantly, non-cancerous HEK293T and PBMC cells displayed generally lower predicted sensitivity compared with cancer cell lines, suggesting the presence of a potential therapeutic window and reduced nonspecific cytotoxicity.

Notably, these computational findings are consistent with experimental observations, who demonstrated that 6,6′-methoxygossypol, 6-methoxygossypol, and apogossypol exerted stronger anticancer activity than gossypol in MCF-7, Caco-2, and SiHa, and LNCaP cells (Wang et al., 2008; Zhan et al., 2015). This concordance between computational predictions and prior experimental data further supports the reliability of the present model and reinforces the potential of methoxylated gossypol derivatives as optimized anticancer scaffolds.

Table 3. Gossypol and its derivatives predicted half-maximal concentration (pIC_{50})

Cancer Type	Compound pIC_{50}									
	GP	6-MGP	HGP	DMGP	6-MHGP	6-DHMGP	AHGP	APGP	GPO	SUN
Breast Cancer										
MCF7	5.11	5.16	4.80	5.19	5.11	4.80	5.10	4.69	5.33	4.89
T47D	6.26	6.23	6.08	6.24	6.11	6.04	5.31	5.66	5.86	5.92
ZR-75-1	5.52	5.88	5.25	6.48	5.79	5.38	5.98	5.46	5.77	6.79
Colorectal Cancer										
Caco-2	4.71	4.75	4.72	4.72	4.76	4.69	4.96	4.77	4.83	5.26
COLO205	5.82	6.06	5.53	6.10	5.47	5.44	5.59	5.90	5.96	5.09

Cancer Type	Compound pIC_{50}									
	GP	6-MGP	HGP	DMGP	6-MHGP	6-DHMGP	AHGP	APGP	GPO	SUN
HCT-8	5.24	5.82	5.52	5.92	6.16	5.42	5.80	5.63	5.34	5.46
SW-620	4.78	5.06	4.68	5.26	4.81	5.01	5.57	5.12	5.76	5.21
Liver Cancer										
HepG2	5.24	5.22	5.12	5.26	5.22	4.95	5.30	5.19	5.42	4.87
Non-cancerous										
HEK293T	4.68	4.75	4.67	4.73	4.63	4.64	4.63	4.84	4.63	5.14
PBMC	5.28	4.98	5.12	5.04	5.41	5.16	4.95	5.15	5.55	4.78

pIC_{50}: Predicted Half-maximum inhibitory concentration; GP: Gossypol; 6-MGP: 6-Methoxygossypol; HGP: Hemigossypol; DMGP: 6,6'-Methoxygossypol; 6-MHGP: 6-Methoxyhemigossypol; 6-DHMGP: 6-Deoxyhemigossypol; AHGP: Anhydrogossypol; APGP: Apogossypol; GPO: Gossypolone; SUN: Sunitinib.

Selectivity index (SI) values calculated using HEK293T and PBMC cells are presented in **Table 4**. Several derivatives exhibited SI values close to or exceeding unity, particularly in colorectal cancer models, indicating preferential cytotoxicity toward cancer cells. Apogossypol and anhydrogossypol demonstrated improved selectivity compared with gossypol, while 6,6′-methoxygossypol combined strong potency with moderate selectivity. Although some SI values were below averages, this behavior is common for multitarget natural products and may be improved through further optimization (Pöhner et al., 2022).

In breast cancer models, most compounds demonstrated SI values ≥ 1.0, particularly against T47D and ZR-75-1 cells. Notably, 6,6′-methoxygossypol displayed consistently high selectivity across both HEK293T and PBMC references, especially against ZR-75-1 cells (SI= 1.37 and 1.29, respectively), surpassing gossypol and approaching or exceeding the selectivity of sunitinib. Gossypolone also showed favorable selectivity against MCF-7 cells (SI= 1.15), suggesting that oxidative modification of the gossypol scaffold may reduce nonspecific cytotoxicity while preserving anticancer activity. In contrast, apogossypol exhibited comparatively lower selectivity in breast cancer models, indicating that removal of aldehyde groups alone may not be sufficient to maximize tumor specificity in this context.

Selectivity trends were particularly pronounced in colorectal cancer cell lines. Several derivatives, including 6,6′-methoxygossypol, anhydrogossypol, and

gossypolone, demonstrated SI values consistently above unity against COLO205, HCT-8, and SW-620 cells. Anhydrogossypol showed robust selectivity across multiple colorectal models, with SI values reaching 1.25-1.21 (HCT-8) and 1.20–1.13 (SW-620), suggesting an improved therapeutic window relative to the parent compound. These findings are notable given the frequent resistance of colorectal cancers to conventional therapies and suggest that optimized gossypol derivatives may preferentially target malignant cells while sparing normal tissues.

In HepG2 liver cancer cells, most compounds exhibited moderate but consistent selectivity, with SI values generally ranging from 1.07 to 1.17. Gossypolone again emerged as one of the more selective derivatives (SI= 1.17), while sunitinib showed comparatively lower selectivity toward cancer cells relative to PBMCs. The modest selectivity observed across all compounds in this model may reflect the high metabolic activity of hepatic cells, which can limit differential cytotoxic responses between cancerous and non-cancerous tissues.

The selectivity index analysis indicates that rational structural modification of gossypol can enhance cancer cell preference, particularly in breast and colorectal cancer models. Among the derivatives, 6,6′-methoxygossypol, anhydrogossypol, and gossypolone consistently demonstrated favorable selectivity profiles across multiple cancer types, often outperforming the parent compound and, in some cases, the reference drug sunitinib. These improvements in selectivity, together with previously observed enhancements in drug-likeness and anticancer potency, suggest a broader therapeutic window for these derivatives.

JURNAL BIOSENSE
Jurnal Penelitian Biologi dan Terapannya
Volume 9 No. 1, Januari 2026, Hal 171 - 194 E-ISSN: 2622 - 6286

Table 4. Gossypol and its derivatives selectivity index (SI) prediction

Cancer Type	Predictive SI of HEK293T and PBMC									
	GP	6-MGP	HGP	DMGP	6-MHGP	6-DHMGP	AHGP	APGP	GPO	SUN
Breast Cancer										
MCF-7	1.09, 0.97	1.09, 1.04	1.03, 0.94	1.10, 1.03	1.10, 0.94	1.03, 0.93	1.10, 1.03	0.97, 0.91	1.15, 0.96	0.95, 1.02
T47D	1.34, 1.19	1.31, 1.25	1.30, 1.19	1.32, 1.24	1.32, 1.13	1.30, 1.17	1.15, 1.07	1.17, 1.10	1.27, 1.06	1.15, 1.24
ZR-75-1	1.18, 1.05	1.24, 1.18	1.12, 1.03	1.37, 1.29	1.25, 1.07	1.16, 1.04	1.29, 1.21	1.13, 1.06	1.25, 1.04	1.32, 1.42
Colorectal Cancer										
Caco-2	1.01, 0.89	1.00, 0.95	1.01, 0.92	1.00, 1.03	1.03, 0.88	1.01, 0.91	1.07, 1.00	0.99, 0.93	1.04, 0.87	1.02, 1.10
COLO205	1.24, 1.10	1.28, 1.22	1.18, 1.08	1.29, 1.21	1.18, 1.01	1.17, 1.05	1.21, 1.13	1.22, 1.15	1.29, 1.07	0.99, 1.06
HCT-8	1.12, 0.99	1.23, 1.17	1.18, 1.08	1.25, 1.17	1.33, 1.14	1.17, 1.05	1.25, 1.17	1.16, 1.09	1.15, 0.96	1.06, 1.14
SW-620	1.02, 0.91	1.07, 1.02	1.00, 0.91	1.11, 1.04	1.04, 0.89	1.08, 0.97	1.20, 1.13	1.06, 0.99	1.24, 1.04	1.01, 1.09
Liver Cancer										
HepG2	1.12, 0.99	1.10, 1.05	1.10, 1.00	1.11, 1.04	1.13, 0.96	1.07, 0.96	1.14, 1.07	1.07, 1.01	1.17, 0.98	0.95, 1.02

GP: Gossypol; 6-MGP: 6-Methoxygossypol; HGP: Hemigossypol; DMGP: 6,6'-Methoxygossypol; 6-MHGP: 6-Methoxyhemigossypol; 6-DHMGP: 6-Deoxyhemigossypol; AHGP: Anhydrogossypol; APGP: Apogossypol; GPO: Gossypolone; SUN: Sunitinib.

3.3 Target prediction and clinical relevance

PASS-based target prediction identified 3-methyladenine DNA glycosylase (MPG) as a high-confidence molecular target for most gossypol derivatives, with probability of activity (Pa) values exceeding 0.90 (**Table 5**). MPG is a key enzyme in the base excision repair (BER) pathway, where it initiates repair of alkylated and damaged DNA bases, thereby maintaining genomic integrity (Kladova & Kuznetsova, 2025). Dysregulated or elevated MPG expression has been reported in several malignancies and is frequently associated with enhanced DNA repair capacity, therapeutic resistance, and unfavorable clinical outcomes (Agnihotri et al., 2014; Barry et al., 2025; Trivedi et al., 2008).

The identification of MPG as a putative target is particularly relevant in the context of anticancer therapy, as inhibition of BER components can sensitize cancer cells to endogenous and therapy-induced DNA damage. Notably, gossypol and its derivative named apogossypol have previously been shown to disrupt key cancer cell survival

pathways, including inhibition of anti-apoptotic Bcl-2 family proteins such as Bcl-2 and Bcl-XL (Huang et al., 2010; Ni et al., 2013; Wei, Kitada, et al., 2009; Zhan et al., 2015).

These observations suggest that gossypol derivatives may exert anticancer activity through dual mechanisms, involving both inhibition of DNA repair via MPG and suppression of anti-apoptotic signaling pathways. This multitarget mode of action is consistent with the broad-spectrum anticancer activity observed in the present study and further supports MPG as a biologically plausible and therapeutically relevant target for optimized gossypol-based compounds.

Table 5. The most feasible predicted target protein of gossypol and its derivatives

Compound Name	Protein Code	Protein Name	Pa[a]	Pi[b]	IAP[c]
Gossypol	MCL1	Myeloid cell leukemia 1	0.723	0.002	0.990
	RSG17	Regulator of G-protein Signaling 17	0.547	0.056	0.877
	MPG	3-methyladenine DNA glycosylase	0.917	0.001	0.976
6-Methoxygossypol	MCL1	Myeloid cell leukemia 1	0.644	0.002	0.990
	HSP10	Heat Shock Protein 10	0.616	0.006	0.958
	ALOX12	Arachidonate 12-Lipoxygenase	0.577	0.019	0.904
	ALOX15	Arachidonate 15-Lipoxygenase	0.567	0.044	0.878
Hemigossypol	MPG	3-methyladenine DNA glycosylase	0.978	0.000	0.976
	RSG17	Regulator of G-protein Signaling 17	0.791	0.007	0.877
	ALOX15	Arachidonate 15-Lipoxygenase	0.783	0.014	0.878
	HSP10	Heat Shock Protein 10	0.775	0.002	0.958
	NEK6	NIMA Related Kinase 6	0.762	0.002	0.968
6,6'-Methoxygossypol	MPG	3-methyladenine DNA glycosylase	0.917	0.001	0.976
	MCL1	Myeloid cell leukemia 1	0.644	0.002	0.990
	HSP10	Heat Shock Protein 10	0.616	0.006	0.958
	ALOX12	Arachidonate 12-Lipoxygenase	0.577	0.019	0.904
	ALOX15	Arachidonate 15-Lipoxygenase	0.567	0.044	0.878

Compound Name	Protein Code	Protein Name	Pa[a]	Pi[b]	IAP[c]
6-Methoxyhemigossypol	MPG	3-methyladenine DNA glycosylase	0.958	0.001	0.976
	ALOX12	Arachidonate 12-Lipoxygenase	0.822	0.005	0.904
	ALOX15	Arachidonate 15-Lipoxygenase	0.795	0.012	0.878
	HSP10	Heat Shock Protein 10	0.735	0.003	0.958
	PKN1	Protein Kinase N1	0.731	0.002	0.871
6-Deoxyhemigossypol	MPG	3-methyladenine DNA glycosylase	0.971	0.001	0.976
	RSG17	Regulator of G-protein Signaling 17	0.752	0.012	0.877
	HSP10	Heat Shock Protein 10	0.735	0.003	0.958
	PKN1	Protein Kinase N1	0.733	0.002	0.871
	SERCA3	Sarco/Endoplasmic Reticulum Calcium ATPase 3	0.669	0.013	0.960
Anhydrogossypol	ALOX15	Arachidonate 15-Lipoxygenase	0.934	0.004	0.878
	MPG	3-methyladenine DNA glycosylase	0.920	0.001	0.976
	RSG17	Regulator of G-protein signaling 17	0.904	0.002	0.877
	HSD17B10	3-hydroxyacyl-CoA dehydrogenase type-2	0.883	0.007	0.878
	ALOX12	Arachidonate 12-Lipoxygenase	0.867	0.004	0.904
Apogossypol	MCL1	Myeloid cell leukemia 1	0.751	0.002	0.990
	RSG17	Regulator of G-protein signaling 17	0.637	0.031	0.877
	ALOX15	Arachidonate 15-Lipoxygenase	0.589	0.040	0.878
	HSD17B10	3-hydroxyacyl-CoA dehydrogenase type-2	0.542	0.055	0.878
	BLM	Bloom syndrome RecQ-like helicase	0.424	0.079	0.854
Gossypolone	MPG	3-methyladenine DNA glycosylase	0.971	0.001	0.976
	MCL1	Myeloid cell leukemia 1	0.905	0.001	0.990
	ALOX15	Arachidonate 15-Lipoxygenase	0.853	0.008	0.878
	RSG17	Regulator of G-protein signaling 17	0.825	0.005	0.904

JURNAL BIOSENSE
Jurnal Penelitian Biologi dan Terapannya
Volume 9 No. 1, Januari 2026, Hal 171 - 194 E-ISSN: 2622 - 6286

Compound Name	Protein Code	Protein Name	Pa[a]	Pi[b]	IAP[c]
	NEK6	NIMA Related Kinase 6	0.808	0.001	0.968

[a]Pa (probability "to be active"): chance that the studied compound is belonging to the sub-class of active compounds; [b]Pi (probability "to be inactive"): chance that the studied compound is belonging to the sub-class of inactive compounds; [c]IAP (invariant accuracy of prediction: the average accuracy of prediction that is obtained for the whole PASS training set in leave-one-out cross-validation procedure.

Importantly, the clinical relevance of MPG targeting is supported by prognostic analysis (**Figure 2**), which demonstrates a significant relationship among MPG high expression and unfavorable overall survival in kidney renal clear cell carcinoma. Furthermore, expression profiling (**Figure 3**) revealed high MPG expression across colorectal, breast, and lung cancers. These clinical relevancy provides compelling support for the therapeutic targeting of MPG and justify further investigation of MPG-directed inhibitors in cancer treatment.

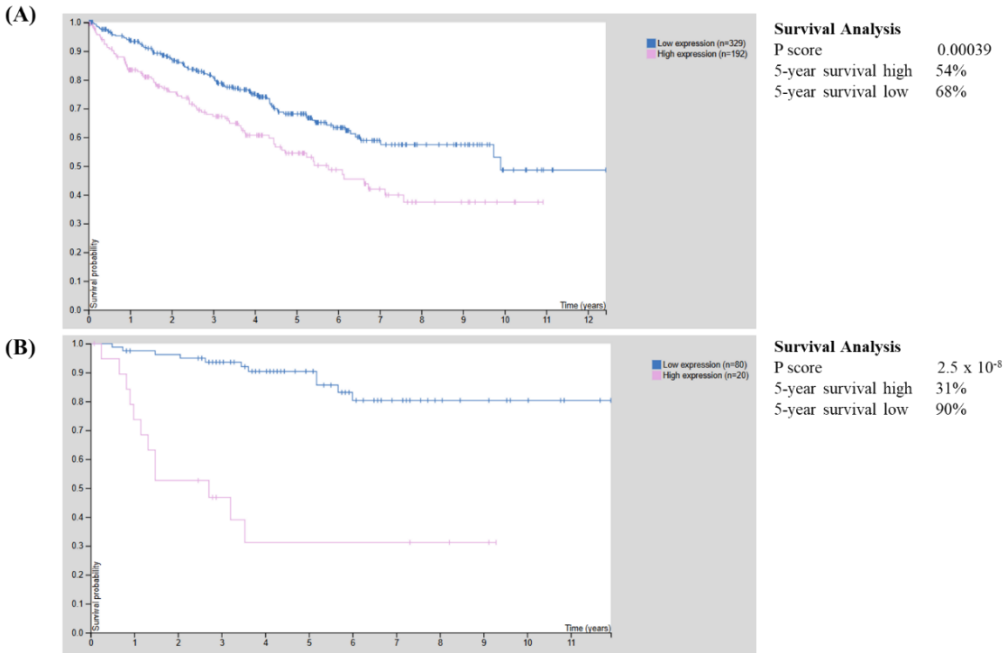

Figure 2. Validated prognostic analysis indicates that increased MPG expression correlates with unfavorable survival in kidney renal clear cell carcinoma, **(A)** TCGA and **(B)** validation.

JURNAL BIOSENSE
Jurnal Penelitian Biologi dan Terapannya
Volume 9 No. 1, Januari 2026, Hal 171 - 194 E-ISSN: 2622 - 6286

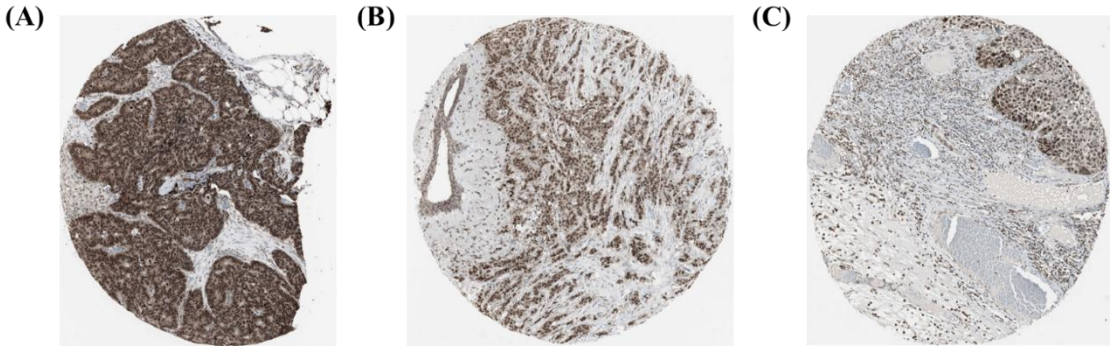

Figure 3. MPG strong expression of patient cancer tissues, **(A)** Colorectal cancer, **(B)** Breast cancer, and **(C)** Lung cancer (retrieved from https://proteinatlas.org).

3.4 Molecular docking and binding interaction analysis

In order to investigate whether gossypol and its derivatives are potent in MPG regulation, we performed molecular docking of gossypol and its derivatives on MPG's structure (PDB ID: 7XFH). The molecular docking study revealed that anhydrogossypol exhibited the strongest binding affinity and the lowest inhibition constant/Ki (-7.55 kcal/mol; Ki= 2.92 µM), followed closely by gossypolone (-7.48 kcal/mol; Ki= 3.30 µM) (**Table 6**). Interestingly, sunitinib showed weaker binding affinity (-5.15 kcal/mol, 169.06 µM) while compared to anhydrogossypol and gossypolone. This finding indicates that both compounds have promising potency as MPG inhibitors. Nevertheless, experimental validation is necessary to prove present findings.

The native compound gossypol demonstrated a moderate binding affinity of -6.33 kcal/mol with an inhibition constant of 22.73 µM. It seemed structural modifications influenced binding performance, as seen with apogossypol (-6.63 kcal/mol; Ki= 13.90 µM), which indicated improvement affinity relative to gossypol. In contrast, methoxy substitutions including 6-methoxygossypol and 6,6'-methoxygossypol caused slightly binding affinity reduction (-5.98 and -6.04 kcal/mol, respectively). Moreover, hemigossypol. 6-methoxyhemigossypol, and 6-deoxyhemigossypol exhibited the weakest interaction, with binding affinities around -4.81 to -4.82 kcal/mol and high

inhibition constants (~295-298 µM).

Table 6. Binding affinity and inhibition constant of gossypol and its derivatives on MPG structure (PDB ID: 7XFH)

No	Compound Name	Binding Affinity (kcal/mol)	Inhibition Constant (µM)	Residual Interaction
1	Gossypol	-6.33	22.73	ILE-161, ARG-182, SER-216, PRO-218, LYS-220
2	6-Methoxygossypol	-5.98	41.30	ILE-161, CYS-167, ARG-182, SER-216, PRO-218
3	Hemigossypol	-4.81	297.69	TYR-162, TYR-165, SER-219
4	6,6'-Methoxygossypol	-6.04	37.68	ILE-161, ARG-182, SER-216, PRO-218, SER-286
5	6-Methoxyhemigossypol	-4.81	296.06	TYR-165, ARG-182, SER-216, GLY-217, PRO-218, LYS-220, SER-286
6	6-Deoxyhemigossypol	-4.82	294.87	TYR-127, ARG-182, VAL-262, VAL-264
7	Anhydrogossypol	-7.55	2.92	TYR-127, ILE-161, TYR-165, CYS-167, ARG-182, SER-216, PRO-218, LYS-220, SER-286
8	Apogossypol	-6.63	13.90	TYR-159, ILE-161, CYS-167, ARG-182, SER-216, PRO-218, SER-219, LYS-220
9	Gossypolone	-7.48	3.30	ALA-134, GLY-163, CYS-167, ARG-182, PRO-218, SER-219
10	Sunitinib	-5.15	169.06	TYR-127, ALA-134, HIS-136, ILE-161, CYS-167, GLY-217, PRO-218, LYS-220

Through docking visualization, we observed that anhydrogossypol interacted with several interacting residues (**Figure 4**). According to prior studies, TYR-127, TYR-165, and CYS-167 were found as highly conserved residues which play crucial roles in DNA base stabilization, substrate recognition and DNA damage discrimination (Chen et al., 2008). In addition, ARG-182 residue has a function in stabilizing the transition state and reaction geometry by interacting with active-site water and DNA phosphate backbone (Lau et al., 2000). Taken together, the engagement of these conserved and catalytically relevant residues suggests that anhydrogossypol may interfere with MPG-mediated DNA repair by stabilizing within the active-site environment.

JURNAL BIOSENSE
Jurnal Penelitian Biologi dan Terapannya
Volume 9 No. 1, Januari 2026, Hal 171 - 194 E-ISSN: 2622 - 6286

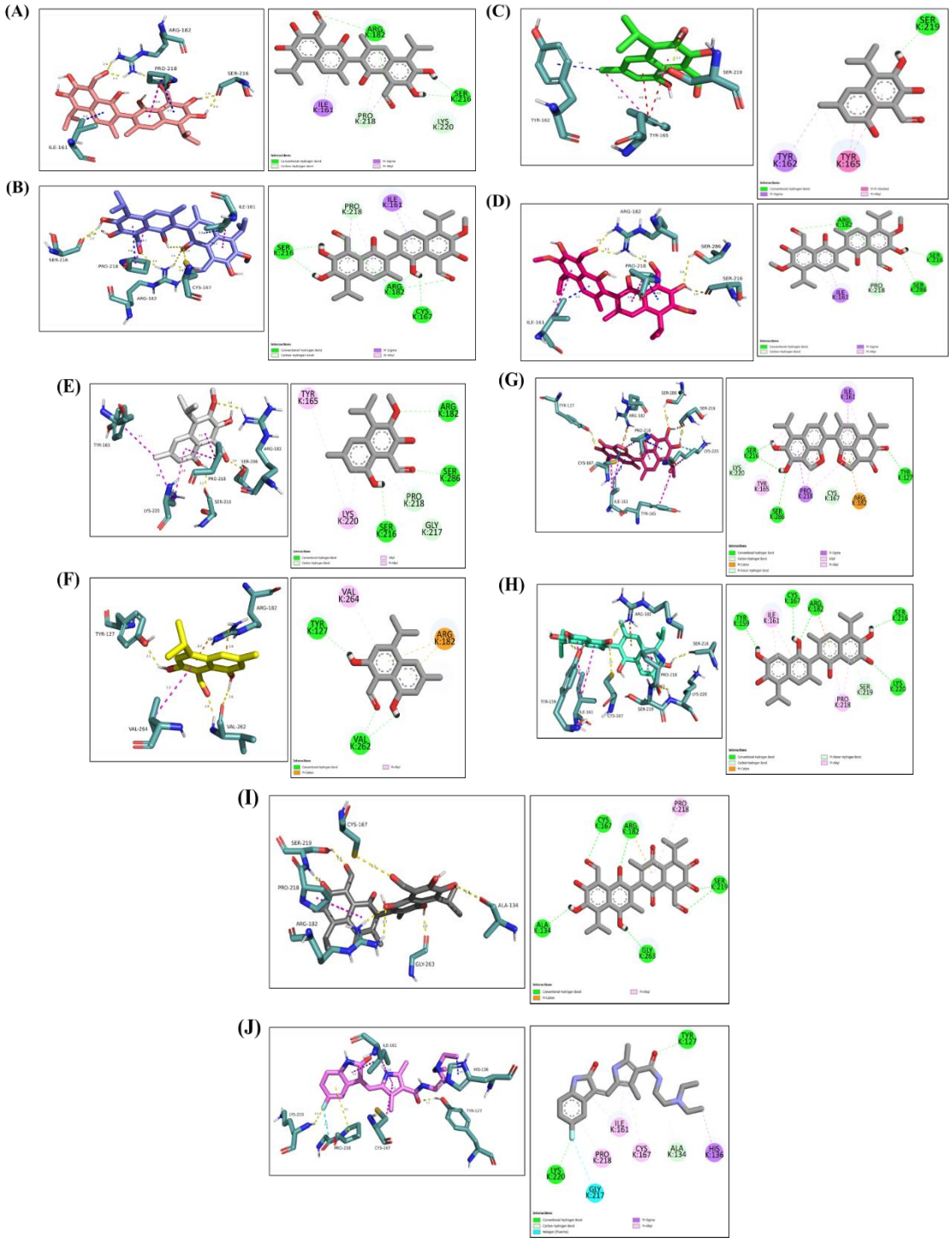

Figure 4. Gossypol and its derivatives binding possibilities with MPG structure, **(A)** GP, **(B)** 6-MGP, **(C)** HGP, **(D)** DMGP, **(E)** 6-MHGP, **(F)** 6-DHMGP, **(G)** AHGP, **(H)** APGP, **(I)** GPO, and **(J)** Sunitinib (positive control).

4. CONCLUSION AND RECOMMENDATIONS

4.1 Conclusion

This study used an integrated computational approach to predict the anticancer potential of gossypol and its derivatives and to identify their cancer target proteins. Several derivatives, particularly anhydrogossypol and gossypolone, demonstrated improved drug-likeness, favorable predicted anticancer activity, and strong binding affinity toward DNA-3-methyladenine glycosylase (MPG). Molecular docking revealed interactions with conserved and functionally important residues involved in substrate recognition and catalytic foster, including TYR-127, TYR-165, CYS-167, and ARG-182. These findings highlight that gossypol derivatives may exert anticancer effects by modulation MPG-mediated DNA repair pathways.

4.2 Recommendations

Further validation through *in vitro* and *in vivo* studies is necessary to confirm MPG inhibition and anticancer efficacy of the identified lead compounds. Enzymatic assays, cellular DNA damage analyses, and mutational studies targeting key residues are strongly recommended. Additionally, combination strategies involving MPG downregulation and DNA-damaging agents should be explored to enhance therapeutic effectiveness.

5. REFERENCES

Agnihotri, S., Burrell, K., Buczkowicz, P., Remke, M., Golbourn, B., Chornenkyy, Y., Gajadhar, A., Fernandez, N. A., Clarke, I. D., Barszczyk, M. S., Pajovic, S., Ternamian, C., Head, R., Sabha, N., Sobol, R. W., Taylor, M. D., Rutka, J. T., Jones, C., Dirks, P. B., … Hawkins, C. (2014). ATM Regulates 3-Methylpurine-DNA Glycosylase and Promotes Therapeutic Resistance to Alkylating Agents. *Cancer Discovery*, *4*(10), 1198–1213. https://doi.org/10.1158/2159-8290.CD-14-0157

Ahmad, I., Kuznetsov, A. E., Pirzada, A. S., Alsharif, K. F., Daglia, M., & Khan, H. (2023). Computational pharmacology and computational chemistry of 4-hydroxyisoleucine: Physicochemical, pharmacokinetic, and DFT-based approaches. *Frontiers in Chemistry*, *11*, 1145974. https://doi.org/10.3389/fchem.2023.1145974

Alhmoud, J. F., Woolley, J. F., Al Moustafa, A.-E., & Malki, M. I. (2020). DNA Damage/Repair Management in Cancers. *Cancers*, *12*(4), 1050. https://doi.org/10.3390/cancers12041050

Banerjee, P., Kemmler, E., Dunkel, M., & Preissner, R. (2024). ProTox 3.0: A webserver for the prediction of toxicity of chemicals. *Nucleic Acids Research*, *52*(W1), W513–W520. https://doi.org/10.1093/nar/gkae303

Barry, C., Shahi, A., & Kidane, D. (2025). DNA glycosylase (NEIL3) overexpression associated with low tumor immune infiltration and poor overall patient survival in endometrial cancer. *Scientific Reports*, *15*(1), 16308. https://doi.org/10.1038/s41598-025-00393-9

Bell, A., Stipanovic, R. D., Howell, C. R., & Fryxell, P. A. (1975). ANTIMICROBIAL TERPENOIDS OF GOSSYPIUM: HEMIGOSSYPOL, 6-METHOXYHEMIGOSSYPOL AND 6-DEOXYHEMIGOSSYPOL. *Phytochemistry*, *14*, 225–231.

Bray, F., Laversanne, M., Sung, H., Ferlay, J., Siegel, R. L., Soerjomataram, I., & Jemal, A. (2024). Global cancer statistics 2022: GLOBOCAN estimates of incidence and mortality worldwide for 36 cancers in 185 countries. *CA: A Cancer Journal for Clinicians*, *74*(3), 229–263. https://doi.org/10.3322/caac.21834

Chen, C., Guo, H., Shah, D., Blank, A., Samson, L., & Loeb, L. (2008). Substrate binding pocket residues of human alkyladenine-DNA glycosylase critical for methylating agent survival. *DNA Repair*, *7*(10), 1731–1745. https://doi.org/10.1016/j.dnarep.2008.06.019

Dao, V. (2000). Synthesis and cytotoxicity of gossypol related compounds. *European Journal of Medicinal Chemistry*, *35*(9), 805–813. https://doi.org/10.1016/S0223-5234(00)00165-3

Elkattan, H. H., Elsisi, A. E., & El-Lakkany, N. M. (2025). Gossypol enhances ponatinib's cytotoxicity against human hepatocellular carcinoma cells by involving cell cycle arrest, p-AKT/LC3II/p62, and Bcl2/caspase-3 pathways. *Toxicology Reports*, *14*, 101856. https://doi.org/10.1016/j.toxrep.2024.101856

Faisal, M., Graidist, P., & Tipmanee, V. (2024). Identification of promising cancer target proteins of major sesquiterpene lactones from *Vernonia* spp. *Journal of Biomolecular Structure and Dynamics*, 1–12. https://doi.org/10.1080/07391102.2024.2446662

Fu, L., Shi, S., Yi, J., Wang, N., He, Y., Wu, Z., Peng, J., Deng, Y., Wang, W., Wu, C., Lyu, A., Zeng, X., Zhao, W., Hou, T., & Cao, D. (2024). ADMETlab 3.0: An updated comprehensive online ADMET prediction platform enhanced with broader coverage, improved performance, API functionality and decision support. *Nucleic Acids Research*, *52*(W1), W422–W431. https://doi.org/10.1093/nar/gkae236

Gadelha, I. C. N., Fonseca, N. B. S., Oloris, S. C. S., Melo, M. M., & Soto-Blanco, B. (2014). Gossypol Toxicity from Cottonseed Products. *The Scientific World Journal*, *2014*, 1–11. https://doi.org/10.1155/2014/231635

Hanwell, M. D., Curtis, D. E., Lonie, D. C., Vandermeersch, T., Zurek, E., & Hutchison, G. R. (2012). Avogadro: An advanced semantic chemical editor, visualization, and analysis platform. *Journal of Cheminformatics*, *4*(1), 17. https://doi.org/10.1186/1758-2946-4-17

Huang, L., Hu, J., Tao, W., Li, Y., Li, G., Xie, P., Liu, X., & Jiang, J. (2010). Gossypol inhibits phosphorylation of Bcl-2 in human leukemia HL-60 cells. *European Journal of Pharmacology*, *645*(1–3), 9–13. https://doi.org/10.1016/j.ejphar.2010.06.070

Kladova, O. A., & Kuznetsova, A. A. (2025). The Link Between Human Alkyladenine DNA

Glycosylase and Cancer Development. *International Journal of Molecular Sciences*, *26*(15), 7647. https://doi.org/10.3390/ijms26157647

Koirala, M., & DiPaola, M. (2024). Overcoming Cancer Resistance: Strategies and Modalities for Effective Treatment. *Biomedicines*, *12*(8), 1801. https://doi.org/10.3390/biomedicines12081801

Lagunin, A. A., Rudik, A. V., Pogodin, P. V., Savosina, P. I., Tarasova, O. A., Dmitriev, A. V., Ivanov, S. M., Biziukova, N. Y., Druzhilovskiy, D. S., Filimonov, D. A., & Poroikov, V. V. (2023). CLC-Pred 2.0: A Freely Available Web Application for In Silico Prediction of Human Cell Line Cytotoxicity and Molecular Mechanisms of Action for Druglike Compounds. *International Journal of Molecular Sciences*, *24*(2), 1689. https://doi.org/10.3390/ijms24021689

Lagunin, A. A., Sezganova, A. S., Muraviova, E. S., Rudik, A. V., & Filimonov, D. A. (2024). BC CLC-Pred: A freely available web-application for quantitative and qualitative predictions of substance cytotoxicity in relation to human breast cancer cell lines. *SAR and QSAR in Environmental Research*, *35*(1), 1–9. https://doi.org/10.1080/1062936X.2023.2289050

Lan, L., Appelman, C., Smith, A. R., Yu, J., Larsen, S., Marquez, R. T., Liu, H., Wu, X., Gao, P., Roy, A., Anbanandam, A., Gowthaman, R., Karanicolas, J., De Guzman, R. N., Rogers, S., Aubé, J., Ji, M., Cohen, R. S., Neufeld, K. L., & Xu, L. (2015). Natural product (−)-gossypol inhibits colon cancer cell growth by targeting RNA-binding protein Musashi-1. *Molecular Oncology*, *9*(7), 1406–1420. https://doi.org/10.1016/j.molonc.2015.03.014

Lau, A. Y., Wyatt, M. D., Glassner, B. J., Samson, L. D., & Ellenberger, T. (2000). Molecular basis for discriminating between normal and damaged bases by the human alkyladenine glycosylase, AAG. *Proceedings of the National Academy of Sciences*, *97*(25), 13573–13578. https://doi.org/10.1073/pnas.97.25.13573

Lee, S., Hong, E., Jo, E., Kim, Z.-H., Yim, K. J., Woo, S. H., Choi, Y.-S., & Jang, H.-J. (2022). Gossypol Induces Apoptosis of Human Pancreatic Cancer Cells via CHOP/Endoplasmic Reticulum Stress Signaling Pathway. *Journal of Microbiology and Biotechnology*, *32*(5), 645–656. https://doi.org/10.4014/jmb.2110.10019

Lin. (2009). Gossypol inhibits the growth of MAT-LyLu prostate cancer cells by modulation of TGFβ/Akt signaling. *International Journal of Molecular Medicine*, *24*(01). https://doi.org/10.3892/ijmm_00000208

Lipinski, C. A., Lombardo, F., Dominy, B. W., & Feeney, P. J. (2012). Experimental and computational approaches to estimate solubility and permeability in drug discovery and development settings. *Advanced Drug Delivery Reviews*, *64*, 4–17. https://doi.org/10.1016/j.addr.2012.09.019

Liu, R., Schyman, P., & Wallqvist, A. (2015). Critically Assessing the Predictive Power of QSAR Models for Human Liver Microsomal Stability. *Journal of Chemical Information and Modeling*, *55*(8), 1566–1575. https://doi.org/10.1021/acs.jcim.5b00255

Miller, R. F., & Adams, R. (1937). Structure of Gossypol. IV.[1,2] Anhydrogossypol and its

Derivatives. *Journal of the American Chemical Society*, *59*(9), 1736–1738. https://doi.org/10.1021/ja01288a051

Ni, Z., Dai, X., Wang, B., Ding, W., Cheng, P., Xu, L., Lian, J., & He, F. (2013). Natural Bcl-2 inhibitor (−)– gossypol induces protective autophagy via reactive oxygen species–high mobility group box 1 pathway in Burkitt lymphoma. *Leukemia & Lymphoma*, *54*(10), 2263–2268. https://doi.org/10.3109/10428194.2013.775437

Pöhner, I., Quotadamo, A., Panecka-Hofman, J., Luciani, R., Santucci, M., Linciano, P., Landi, G., Di Pisa, F., Dello Iacono, L., Pozzi, C., Mangani, S., Gul, S., Witt, G., Ellinger, B., Kuzikov, M., Santarem, N., Cordeiro-da-Silva, A., Costi, M. P., Venturelli, A., & Wade, R. C. (2022). Multitarget, Selective Compound Design Yields Potent Inhibitors of a Kinetoplastid Pteridine Reductase 1. *Journal of Medicinal Chemistry*, *65*(13), 9011–9033. https://doi.org/10.1021/acs.jmedchem.2c00232

Sadahira, K., Sagawa, M., Nakazato, T., Uchida, H., Ikeda, Y., Okamoto, S., Nakajima, H., & Kizaki, M. (2014). Gossypol induces apoptosis in multiple myeloma cells by inhibition of interleukin-6 signaling and Bcl-2/Mcl-1 pathway. *International Journal of Oncology*, *45*(6), 2778–2286. https://doi.org/10.3892/ijo.2014.2652

Saraswat, R., Gangawat, L. K., Khardiya, M., & Singh, D. (2022). Medicinal Chemistry In The Path Of Drug Discovery. *Journal of Pharmaceutical Negative Results*, *13*(9). https://doi.org/10.47750/x67j0439

Shah, P., Siramshetty, V. B., Zakharov, A. V., Southall, N. T., Xu, X., & Nguyen, D.-T. (2020). Predicting liver cytosol stability of small molecules. *Journal of Cheminformatics*, *12*(1), 21. https://doi.org/10.1186/s13321-020-00426-7

Song, Y.-Q., Li, G.-D., Niu, D., Chen, F., Jing, S., Wai Wong, V. K., Wang, W., & Leung, C.-H. (2023). A robust luminescent assay for screening alkyladenine DNA glycosylase inhibitors to overcome DNA repair and temozolomide drug resistance. *Journal of Pharmaceutical Analysis*, *13*(5), 514–522. https://doi.org/10.1016/j.jpha.2023.04.010

Stipanovic, R. D., Bell, A. A., Mace, M. E., & Howell, C. R. (1975). Antimicrobial terpenoids of Gossypium: 6-methoxygossypol and 6,6′-dimethoxygossypol. *Phytochemistry*, *14*(4), 1077–1081. https://doi.org/10.1016/0031-9422(75)85190-9

Šudomová, M., & Hassan, S. T. S. (2022). Gossypol from Gossypium spp. Inhibits Helicobacter pylori Clinical Strains and Urease Enzyme Activity: Bioactivity and Safety Assessments. *Scientia Pharmaceutica*, *90*(2), 29. https://doi.org/10.3390/scipharm90020029

Sun, X., Ying, J., Ma, X., Zhong, Y., Huo, R., & Meng, Q. (2025). Effects of Gossypol Exposure on Ovarian Reserve Function: Comprehensive Risk Assessment Based on TRAEC Strategy. *Toxics*, *13*(9), 763. https://doi.org/10.3390/toxics13090763

Trivedi, R. N., Wang, X., Jelezcova, E., Goellner, E. M., Tang, J., & Sobol, R. W. (2008). Human Methyl Purine DNA Glycosylase and DNA Polymerase β Expression Collectively Predict Sensitivity to Temozolomide. *Molecular Pharmacology*, *74*(2), 505–516. https://doi.org/10.1124/mol.108.045112

Veber, D. F., Johnson, S. R., Cheng, H.-Y., Smith, B. R., Ward, K. W., & Kopple, K. D. (2002). Molecular Properties That Influence the Oral Bioavailability of Drug Candidates.

Journal of Medicinal Chemistry, *45*(12), 2615–2623. https://doi.org/10.1021/jm020017n

Wang, X., Beckham, T. H., Morris, J. C., Chen, F., & Gangemi, J. D. (2008). Bioactivities of Gossypol, 6-Methoxygossypol, and 6,6′-Dimethoxygossypol. *Journal of Agricultural and Food Chemistry*, *56*(12), 4393–4398. https://doi.org/10.1021/jf073297u

Wang, Y., Lai, H., Fan, X., Luo, L., Duan, F., Jiang, Z., Wang, Q., Leung, E. L. H., Liu, L., & Yao, X. (2018). Gossypol Inhibits Non-small Cell Lung Cancer Cells Proliferation by Targeting EGFRL858R/T790M. *Frontiers in Pharmacology*, *9*, 728. https://doi.org/10.3389/fphar.2018.00728

Wei, J., Jagt, D. L. V., Royer, R. E., & Deck, L. M. (2010). Synthesis of hemigossypol and its derivatives. *Tetrahedron Letters*, *51*(44), 5757–5760. https://doi.org/10.1016/j.tetlet.2010.08.089

Wei, J., Kitada, S., Rega, M. F., Emdadi, A., Yuan, H., Cellitti, J., Stebbins, J. L., Zhai, D., Sun, J., Yang, L., Dahl, R., Zhang, Z., Wu, B., Wang, S., Reed, T. A., Lawrence, N., Sebti, S., Reed, J. C., & Pellecchia, M. (2009). Apogossypol derivatives as antagonists of antiapoptotic Bcl-2 family proteins. *Molecular Cancer Therapeutics*, *8*(4), 904–913. https://doi.org/10.1158/1535-7163.MCT-08-1050

Wei, J., Rega, M. F., Kitada, S., Yuan, H., Zhai, D., Risbood, P., Seltzman, H. H., Twine, C. E., Reed, J. C., & Pellecchia, M. (2009). Synthesis and evaluation of Apogossypol atropisomers as potential Bcl-xL antagonists. *Cancer Letters*, *273*(1), 107–113. https://doi.org/10.1016/j.canlet.2008.07.031

Wong, F. Y., Liem, N., Xie, C., Yan, F. L., Wong, W. C., Wang, L., & Yong, W.-P. (2012). Combination Therapy with Gossypol Reveals Synergism against Gemcitabine Resistance in Cancer Cells with High BCL-2 Expression. *PLoS ONE*, *7*(12), e50786. https://doi.org/10.1371/journal.pone.0050786

Wu, F., Zhou, Y., Li, L., Shen, X., Chen, G., Wang, X., Liang, X., Tan, M., & Huang, Z. (2020). Computational Approaches in Preclinical Studies on Drug Discovery and Development. *Frontiers in Chemistry*, *8*, 726. https://doi.org/10.3389/fchem.2020.00726

Xiong, J., Li, J., Yang, Q., Wang, J., Su, T., & Zhou, S. (2017). Gossypol has anti-cancer effects by dual-targeting MDM2 and VEGF in human breast cancer. *Breast Cancer Research*, *19*(1), 27. https://doi.org/10.1186/s13058-017-0818-5

Zhan, W., Hu, X., Yi, J., An, Q., & Huang, X. (2015). Inhibitory activity of apogossypol in human prostate cancer in vitro and in vivo. *Molecular Medicine Reports*, *11*(6), 4142–4148. https://doi.org/10.3892/mmr.2015.3326